THE JOURNAL OF BIOLOGICAL CHEMISTRY
Vol. 280, No. 4, Issue of January 28, pp. 2904–2911, 2005
Printed in U.S.A.

Association of NASP with HSP90 in Mouse Spermatogenic Cells

STIMULATION OF ATPase ACTIVITY AND TRANSPORT OF LINKER HISTONES INTO NUCLEI*

Received for publication, September 10, 2004, and in revised form, October 29, 2004
Published, JBC Papers in Press, November 8, 2004, DOI 10.1074/jbc.M410397200

Oleg M. Alekseev, Esther E. Widgren, Richard T. Richardson, and Michael G. O'Rand‡

From the Department of Cell and Developmental Biology, University of North Carolina at Chapel Hill, Chapel Hill, North Carolina 27599-7090

NASP (nuclear autoantigenic sperm protein) is a linker histone-binding protein found in all dividing cells that is regulated by the cell cycle (Richardson, R. T., Batova, I. N., Widgren, E. E., Zheng, L. X., Whitfield, M., Marzluff, W. F., and O'Rand, M. G. (2000) *J. Biol. Chem.* 275, 30378–30386), and in the nucleus linker histones not bound to DNA are bound to NASP (Alekseev, O. M., Bencic, D. C., Richardson R. T., Widgren E. E., and O'Rand, M. G. (2003) *J. Biol. Chem.* 278, 8846–8852). In mouse spermatogenic cells tNASP binds the testis-specific linker histone H1t. Utilizing a cross-linker, 3,3′-dithiobissulfosuccinimidyl propionate, and mass spectrometry, we have identified HSP90 as a testis/embryo form of NASP (tNASP)-binding partner. *In vitro* assays demonstrate that the association of tNASP with HSP90 stimulated the ATPase activity of HSP90 and increased the binding of H1t to tNASP. HSP90 and tNASP are present in both nuclear and cytoplasmic fractions of mouse spermatogenic cells; however, HSP90 bound to NASP only in the cytoplasm. *In vitro* nuclear import assays on permeabilized HeLa cells demonstrate that tNASP, in the absence of any other cytoplasmic factors, transports linker histones into the nucleus in an energy and nuclear localization signal-dependent manner. Consequently we hypothesize that in the cytoplasm linker histones are bound to a complex containing NASP and HSP90 whose ATPase activity is stimulated by binding NASP. NASP-H1 is subsequently released from the complex and translocates to the nucleus where the H1 is released for binding to the DNA.

Linker histones (H1s)[1] bind to DNA in the nucleosomes of chromatin and influence the formation of chromatin fibers, gene transcription, nucleosome spacing, chromatin remodeling, and cell cycle progression (1–5). Studies on linker histones in the cell nucleus indicate that there is a constant exchange of H1s with their DNA-binding sites (6, 7) and that H1s not bound to DNA are bound to the histone-binding protein NASP (8). NASP is a histone-binding protein found in all dividing cells in either a somatic/embryo or testis/embryo (tNASP) form (9–11). Overexpression of tNASP affects progression through the cell cycle, and Alekseev *et al.* (8) recently postulated that a dynamic equilibrium exists between H1-NASP complexes and H1 bound to DNA. Previous studies on NASP (9) demonstrated that *in vivo* the somatic linker histones H1a-H1e (see Ref. 12 for mouse histone H1 nomenclature) were co-precipitated with NASP from somatic cell lysates, indicating that NASP is not selective for H1 subtypes.

Of the several different subtypes of H1 histones, H1a, b, c, d, and e are found in most cells, whereas H1t is restricted to the testis. H1t is expressed during spermatogenesis, representing as much as 50% of the total H1 histones in pachytene spermatocytes (13–15), and is preceded by tNASP expression in preleptotene spermatocytes. Although their exact function during spermatogenesis is unknown, gene-targeting experiments (16) have shown that the absence of H1t and H1a in double null mice does not compromise spermatogenesis because compensation by H1c, H1d, and H1e most likely maintained normal spermatogenesis despite a reduced H1/nucleosome ratio (16). Under these conditions the major H1 histone binding activity of tNASP could have shifted from H1t to H1c, H1d, and H1e in double null mice. Unfortunately neither the relationship between tNASP, H1t, and other proteins nor the ability of tNASP to transport H1s into the mammalian cell nucleus has been characterized. Therefore we have studied tNASP in spermatogenic cells to understand more about the role of NASP-H1t complexes and now report that H1t binds tNASP in mouse germ cells in a complex in the cytoplasm that contains HSP90, which facilitates the initial loading of linker histones to tNASP. Moreover, tNASP can transport both H1t and somatic linker histones into nuclei.

EXPERIMENTAL PROCEDURES

All of the chemicals and reagents used in this study were molecular biology grade. The restriction enzymes were purchased from Roche Applied Science. Purification of plasmid DNA and PCR products were carried out using QIAprep Miniprep and QIAquick PCR purification kits (Qiagen), and sequencing was performed at the University of North Carolina at Chapel Hill automated sequencing facility. Rabbit anti-histone H1 (FL-219) polyclonal antiserum and mouse monoclonal IgG_{2a} anti-HSP90 (F-8) antiserum were purchased from Santa Cruz Biotechnology (Santa Cruz, CA). Anti-H1t antibody was a gift from Dr. M. Meistrich (Department of Experimental Radiation Oncology, M. D. Anderson Cancer Center, University of Texas, Houston, TX). Rabbit antisera to the N terminus of NASP (nucleotides 96–1099) were prepared as described previously (9). Rabbit antisera to full-length recombinant NASP (nucleotides 92–2405) were made by Bethyl Laboratories (Montgomery, TX). Somatic linker histones from calf thymus were purchased from Roche Applied Science.

Construction of Expression Vectors—The entire coding sequence of mouse tNASP (nucleotides 92–2406, GenBank™ accession number AF034610) was amplified from mouse testis Quick-clone cDNA (Clon-

* This work was supported by NICHD, National Institutes of Health through Cooperative Agreement U54HD35041 as part of the Specialized Cooperative Centers Program in Reproductive Research. The costs of publication of this article were defrayed in part by the payment of page charges. This article must therefore be hereby marked "*advertisement*" in accordance with 18 U.S.C. Section 1734 solely to indicate this fact.

‡ To whom correspondence should be addressed: Dept. of Cell & Developmental Biology, CB# 7090, University of North Carolina at Chapel Hill, Chapel Hill, NC 27599-7090. Tel.: 919-966-5698; Fax: 919-966-1856; E-mail: morand@unc.edu.

[1] The abbreviations used are: H1, linker histone; tNASP, testis/embryo form of NASP; HSP90, heat shock protein 90; NLS, nuclear localization signal; H1t, testis form of H1; HPLC, high pressure liquid chromatography; DTSSP, 3,3′-dithiobissulfosuccinimidyl propionate; MALDI, matrix assisted laser desorption/ionization; TOF, time of flight; TPR, tetratricopeptide repeat.

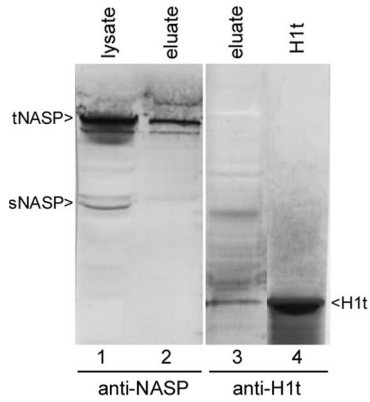

FIG. 1. **Western blot analysis of tNASP and H1t in the eluates from anti-NASP affinity chromatography of mouse testis lysates.** *Lane 1*, mouse testis lysate loaded onto the affinity column, probed with anti-NASP antibodies. *Lane 2*, eluate from the affinity column, probed with anti-NASP antibodies. *Lane 3*, eluate from the affinity column, probed with anti-H1t antibodies. *Lane 4*, reverse phase HPLC-purified mouse H1t probed with anti-H1t antibodies. *sNASP*, somatic/embryo form of NASP.

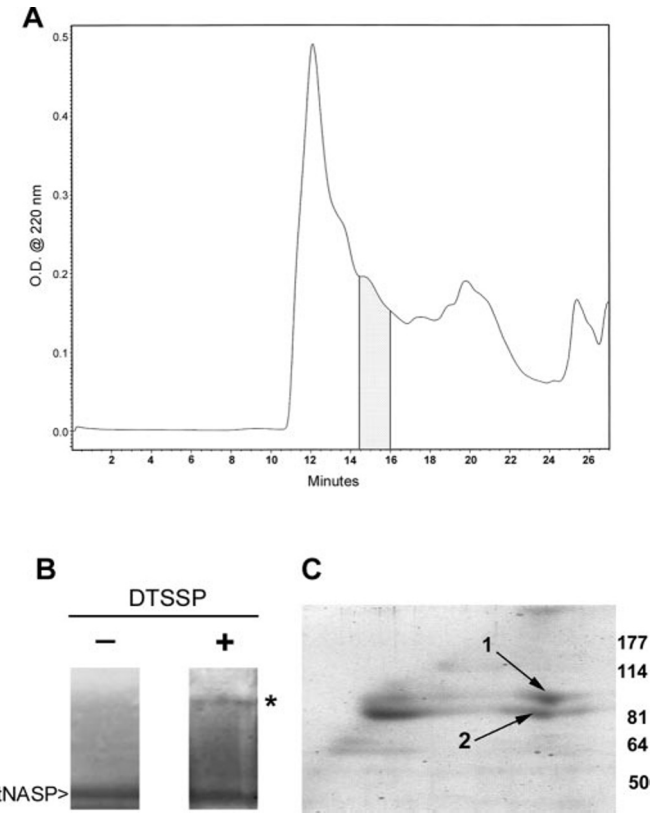

FIG. 2. *A*, size exclusion HPLC separation of tNASP from a mouse testis lysate; fractions (14.5–16 min; patterned area) were identified by Western blotting as NASP-positive fractions. *B*, pooled tNASP-positive fraction separated by nonreducing SDS-PAGE with or without cross-linker DTSSP added to a final concentration of 2 mM. The *asterisk* shows the position of the cross-linked (~200 kDa) tNASP-positive band. *C*, the lane containing cross-linked tNASP was cleaved by incubation in 50 mM dithiothreitol, placed horizontally onto a 10% acrylamide gel, and separated in the second dimension (reducing). Protein staining bands located below the tNASP-positive band (*arrows*) were excised, digested with trypsin, and identified by MALDI-TOF and MALDI-TOF/TOF.

tech, Palo Alto, CA) as described previously (8). A tNASP deletion mutant (NASP-ΔTPR; nucleotides 92–1590), that lacked all tetratricopeptide repeats (nucleotides 1591–1891) was PCR-amplified, cloned into pCR® T7/CT-TOPO vector (Invitrogen), expressed, and purified identically to the full-length construct (8). Preparation of the NLS deletion mutant (NASP-ΔNLS) has been described previously (8).

Isolation, Separation, and Short Term Culture of Spermatogenic Cells—Isolation, separation, and short term culture of spermatogenic cells were carried out as described previously (17, 18). The cells were grown in plastic flasks for 16–18 h to allow Sertoli cells and other somatic cells to adhere to the bottom of the flask, and spermatogenic cells were collected from the supernatant.

Harvested mouse spermatogenic cells were washed in phosphate-buffered saline and Earle's balanced salt solution (5.3 mM KCl, 117 mM NaCl, 26 mM $NaHCO_3$, 1 mM NaH_2PO_4, and 5.6 mM glucose) and resuspended in 10 volumes of RBS buffer (10 mM Tris-HCl, pH 7.4, 10 mM NaCl, 3 mM $MgCl_2$) containing 1 mM phenylmethylsulfonyl fluoride and protease inhibitor mixture (catalog number 8340; Sigma). The nuclei were prepared essentially as described (19). After incubation on ice for 10 min, the cells were transferred to a prechilled glass Dounce-type homogenizer and subjected to 10–12 quick strokes of the pestle. The nuclei were removed from the cytoplasmic fraction by centrifugation at 1000 × *g* for 3 min, washed with phosphate-buffered saline, and sonicated for 20 s. The supernatant (nuclear fraction) was cleared by centrifugation for 10 min at 1000 × *g*. Microscopic examination of the nuclei and Western blotting (staining for histones) of nuclear and cytoplasmic fractions confirmed their separation.

In Vitro Nuclear Transport Assay—The nuclear import assay was performed on permeabilized HeLa cells as described previously (20). The cells were grown on 22 × 22-mm glass coverslips in six-well plates (Corning, Corning, NY) and washed in ice-cold import buffer (20 mM HEPES, pH 7.3, 110 mM potassium acetate, 2 mM magnesium acetate, 1 mM EGTA, 2 mM dithiothreitol, 1 μg/ml each of aprotinin, leupeptin, and pepstatin). The cells were permeabilized in ice-cold import buffer containing 40 μg/ml digitonin (40 mg/ml stock solution in dimethyl sulfoxide; Calbiochem, San Diego, CA) for 8 min. Digitonin containing buffer was replaced by ice-cold import buffer, and the cells were washed in several changes of import buffer for 30 min with gentle rocking. The complete import mixture contained 50% (v/v) cytosol (the cytoplasmic fraction of HeLa cells centrifuged at 60 000 × *g*; total protein concentration was 10 mg/ml), 1 mM adenosine-5′-triphosphate, 5 mM creatine phosphate, 20 units/ml creatine phosphokinase (Calbiochem), and 10 μM biotin-labeled histone H1t. Mouse tNASP or NASP-ΔNLS was added to a final concentration of 5 μM. The coverslips were inverted over 150 μl of complete import mixture on a sheet of parafilm in a humidified plastic box and incubated at 37 °C for 30 min. The transport reaction was stopped by fixation in 3% formaldehyde for 15 min. The coverslips were incubated in Texas Red Avidin D (Vector Laboratories, Burlingame, CA) for 1 h, briefly washed in phosphate-buffered saline, and incubated in 4′,6′-diamino-2-phenylindole nucleic acid stain (Molecular Probes, Eugene, OR) for 2 min. The coverslips were mounted in ProLong Antifade (Molecular Probes) and examined with a Zeiss Axiophot as described previously (21).

Chromatography—Immunoaffinity chromatography was carried out as described previously (8). For the preparation of NASP-enriched fractions from testis, lysates of 50 mouse testes (Pel-Freez® Biologicals, Rogers, AR) were prepared in 2 ml of MPER reagent (Pierce) with Protease (catalog number 8340; Sigma) and Proteasome (catalog number 539160; Calbiochem) inhibitors added. The cells were vortexed thoroughly and rocked for 10 min at room temperature. Debris was removed by centrifugation (10 min, 12,000 rpm), and the supernatant was applied to a 21 × 600-mm Bio-Sep SEC-S 3000 size exclusion HPLC column equipped with a 75 × 21.2-mm precolumn (Phenomenex, Torrance, CA) in 10 mM phosphate buffer, pH 7.0, 252 mM NaCl. 1650 μl were injected per run at a flow rate of 7 ml/min, and fractions were collected every 0.25 min for 27 min. 500-μl aliquots of the collected fractions were concentrated in Amicon (Beverly, MA) microcentrifuge filters (molecular weight cut-off = 10,000 Daltons), boiled with SDS sample buffer containing β-mercaptoethanol, and analyzed by Western blotting. NASP-positive fractions were pooled (see Fig. 2A).

Linker histones were purified from mouse testes (Pel-Freez® Biologicals) according to the method of Brown and Sittman (22). Lyophilized histones were dissolved in 0.1% trifluoroacetic acid and applied to a C-18 reverse phase column (Waters, Milford, MA; Delta-Pak, 15 μm, 300 Å, 3.9 × 300 mm) as described previously (8, 9). H1t fractions were pooled and used for further experiments.

Mass Spectrometry Identification of tNASP-binding Partners—Water-soluble cross-linker 3,3′-dithiobis-(sulfosuccinimidylpropionate (DTSSP; 2 mM; Pierce) with a spacer arm length of 12 Å was added to the Bio-Sep SEC-S 3000 column NASP pooled fraction (described above), incubated (at room temperature for 30 min), and analyzed by nonreducing SDS-PAGE. Western blots probed with anti-NASP antibody identified a high molecular weight NASP-positive band. A strip of

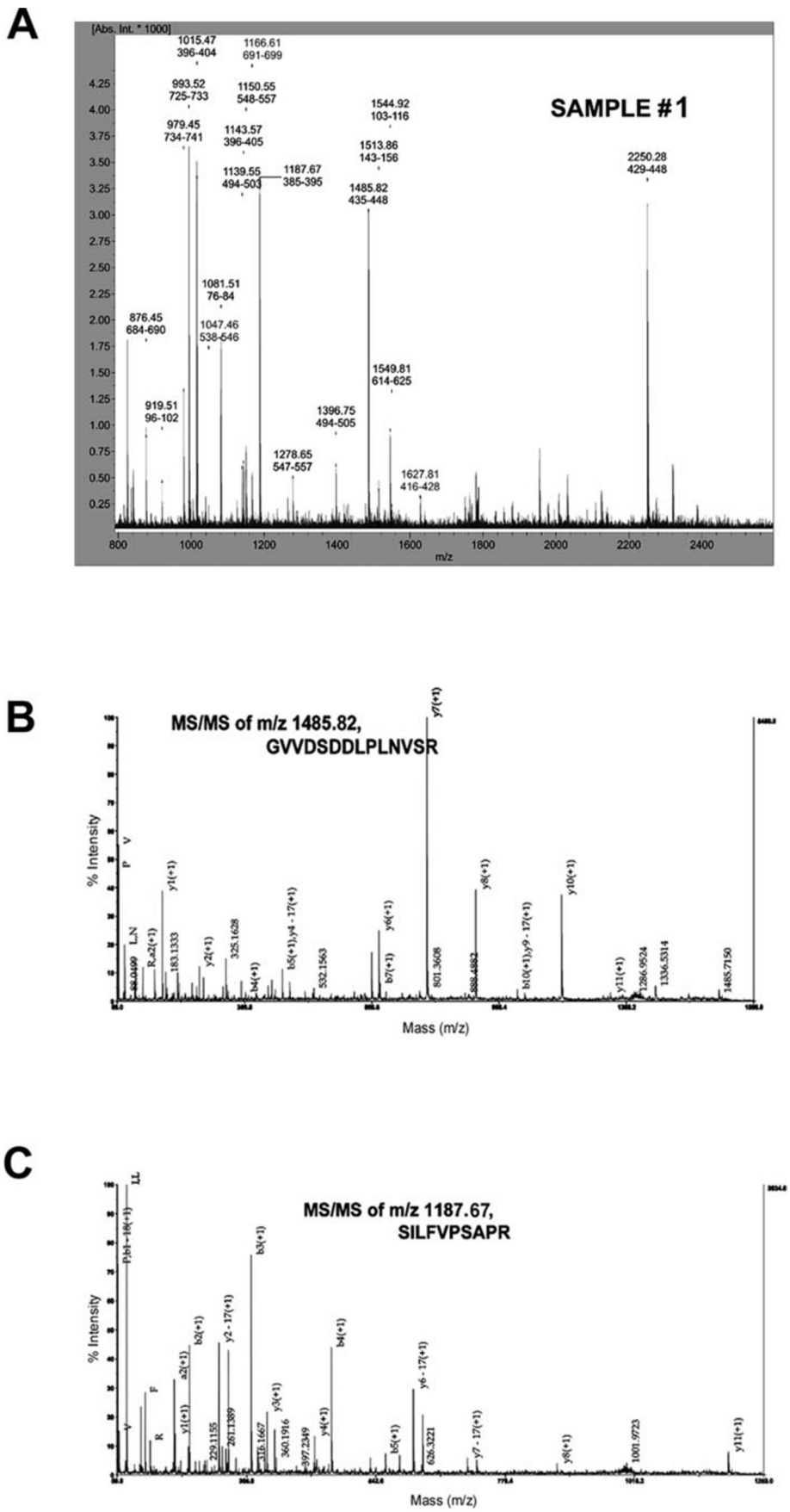

FIG. 3. *A*, MALDI-TOF of tryptic peptides recovered from *sample 1* of the second dimension gel of tNASP binding partners demonstrates peaks typical for tumor rejection antigen gp96. *B* and *C*, two peaks, *m/z* 1485.82 and 1187.67 (from *A*) sequenced by tandem mass spectrometry (MALDI-TOF/TOF) confirmed the tumor rejection antigen gp96 sequence.

gel containing the high molecular weight NASP-positive band was excised from a second identical gel, incubated in 50 mM dithiothreitol (Sigma; at 37 °C for 30 min), placed horizontally into a well of a 10% acrylamide gel (1 mm thick), and separated in the second dimension in the presence of β-mercaptoethanol. The resulting gel was stained by 0.01% Bio-Rad R-250 Coomassie in 10% acetic acid overnight. Protein

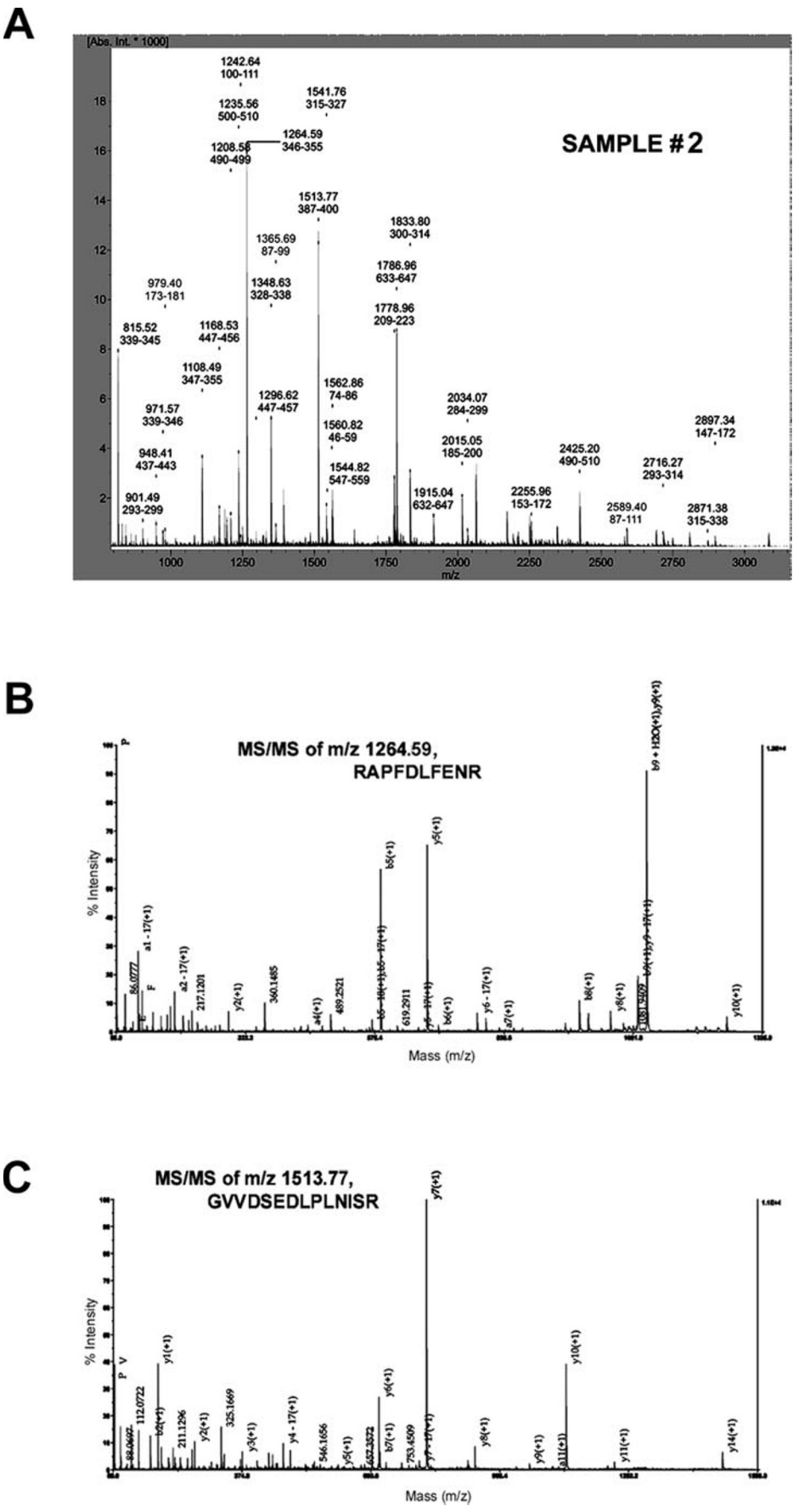

FIG. 4. *A*, MALDI-TOF of tryptic peptides recovered from *sample 2* of the second dimension gel of tNASP-binding partners demonstrates peaks typical for HSP90. *B* and *C*, two peaks, *m/z* 1264.59 and 1513.77 (from *A*) sequenced by tandem mass spectrometry (MALDI-TOF/TOF) confirmed the HSP90 sequence.

staining bands located below the position of the noted high molecular weight NASP-positive band (~200 kDa) were excised and prepared for MALDI-TOF analysis. Digestion of the selected bands was accomplished using the Genomic Solutions ProGest with sequencing grade modified trypsin (Promega, Madison, WI). The resultant peptide solution was then lyophilized and reconstituted in 45% methanol, 45%

water, 10% formic acid. This solution was combined on the MALDI target with a saturated matrix solution of α-cyano-4-hydroxy-cinnamic acid. MALDI-TOF and MALDI-TOF/TOF were performed on the AB 4700 Voyager Proteomics Discovery System (Applied Biosystems, Foster City, CA). The resulting peptide peaks were searched against the MSDB and NCBI databases using the MASCOT search engine of GPS Explorer software. Mass spectrometry identification was done in the University of North Carolina at Chapel Hill Proteomics Core Laboratory.

ATPase Assay—The amount of ATP in solution was detected by the ENLITEN® ATP Assay System Bioluminescence Detection Kit (Promega). Bioluminescence was measured on a TD-20/20 Luminometer (Turner BioSystems, Sunnyvale, CA). The assays were performed in 40 mM HEPES, pH 7.5, 5 mM $MgCl_2$, and 10^{-8} M ATP (Calbiochem). Typical protein concentrations were 0.2 μM for HSP90 and albumin and 0.2 μM for tNASP unless otherwise indicated. The temperature was set to 37 °C. Background (nonspecific) readings were subtracted from the total activity. Relative light units were normalized for comparing the results from different experiments. As ATPase activity increases the relative light units decrease. Significance was determined by the Student's *t* test.

Co-immunoprecipitation—For binding experiments reverse phase HPLC purified H1t was biotin-labeled and mixed with recombinant tNASP (10 μg) in a 500-μl volume of 40 mM HEPES, pH 7.7, 5 mM $MgCl_2$ and incubated for 1 h at 37 °C with gentle shaking. As required by the experiment, HSP90 (2 μg) and/or ATP (1 mM) were added. The precipitations were carried out with affinity-purified rabbit anti-recombinant NASP antibodies. Antibody-protein complexes were collected by Ultra Link® immobilized protein A/G (Pierce) and eluted by boiling in SDS-PAGE sample buffer containing β-mercaptoethanol. The samples were separated in 10–20% SDS-polyacrylamide gels (Bio-Rad) by electrophoresis, and the amount of co-immunoprecipitated H1t was calculated from background-subtracted images using Gel Expert software (Nucleotech, San Carlos, CA).

RESULTS

Association of H1t Histones with tNASP—Isolation of NASP from mouse testis lysates by affinity chromatography with anti-NASP antibodies resulted in co-purification of H1 histones. Previous studies on NASP (9) demonstrated that the somatic linker histones were co-precipitated with NASP. The presence of linker histone H1t was identified by probing Western blots with specific H1t antibody (Fig. 1, *lane 3*). Western blot analysis of the H1t co-purified with tNASP and H1t histones extracted from the mouse testis and isolated by reverse phase HPLC indicated that they had identical SDS-PAGE profiles (Fig. 1, *lane 4*).

Identification of tNASP-binding Partners—To identify additional binding partners that may be complexed with tNASP in mouse germ cells, we used size exclusion chromatography and gel electrophoresis to isolate tNASP complexes. tNASP complexes were identified by SDS-PAGE and Western blot analysis with anti-NASP antibodies following size exclusion HPLC separation of a mouse testis lysate on a Bio-Sep SEC-S 3000 column (Fig. 2*A*). NASP complexes were pooled and cross-linked with DTSSP. Nonreducing SDS-PAGE analysis of the cross-linked complexes indicated the appearance of an ~200-kDa NASP-positive band (Fig. 2*B*, *asterisk*). This cross-linked complex was cleaved by incubation of the gel in dithiothreitol, and the gel lane was subsequently placed horizontally and electrophoresed in the second dimension. Immediately under the reduced NASP complex two major protein-staining bands were revealed (Fig. 2*C*, *bands 1* and *2*).

Initial identification of band 1 by MALDI-TOF (Fig. 3*A*) and additional confirming MALDI-TOF/TOF analysis of its peaks 1485.82 and 1187.67 (Fig. 3, *B* and C) identified this band as an endoplasmic reticulum protein 99 precursor (accession number A29317; tumor rejection antigen gp96). This protein belongs to the heat shock protein 90 family and has a histidine kinase-like ATPase domain. Band 2 (Fig. 2*C*) was identified as mouse heat shock protein 90α (accession number P070901; HSP86-1, tumor-specific transplantation 86-kDa antigen) with MALDI-TOF/TOF analysis of peaks 1264.59 and 1513.77 (Fig. 4). Heat shock protein 90 is a molecular chaperone with ATPase activity.

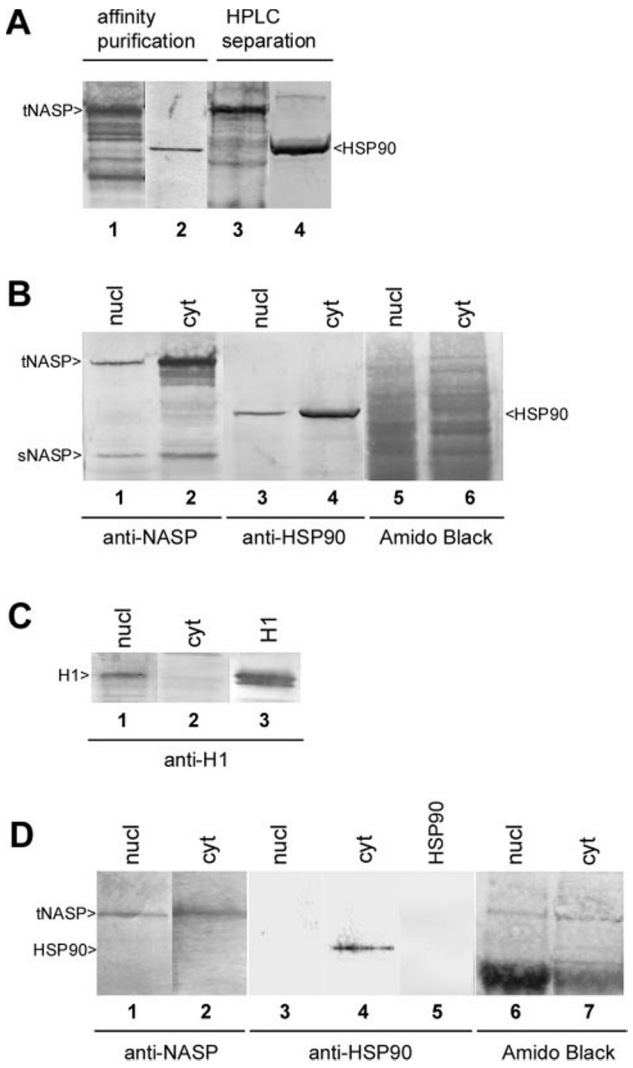

FIG. 5. **Association of tNASP with HSP90 in mouse germ cells.** *A*, *lanes 1* and *2*, eluate from the anti-NASP antibody affinity column loaded with a mouse testis lysate, probed with rabbit anti-NASP antibody (*lane 1*) and anti-HSP90 antibody (*lane 2*). *Lanes 3* and *4*, size exclusion HPLC tNASP-enriched fraction probed with rabbit anti-NASP antibody (*lane 3*) and anti-HSP90 antibody (*lane 4*). *B*, mouse germ cell nuclear and cytoplasmic fractions. *Lanes 1* and *2*, probed with rabbit anti-NASP antibody. *Lanes 3* and *4*, probed with rabbit anti-HSP90 antibody. *Lanes 5* and *6*, Amido Black stain. The lanes were loaded with equal amounts of protein. *C*, mouse germ cell nuclear and cytoplasmic fractions probed with anti-H1 antibody. *Lanes 1* and *2*, no H1 is detected in the cytoplasmic fraction, demonstrating the effectiveness of the separation. *Lane 3*, commercial calf thymus H1 probed with anti-H1 antibody. *D*, eluate from the anti-NASP antibody affinity column loaded with either a mouse testis cytoplasmic or nuclear fraction. *Lanes 1* and *2*, probed with rabbit anti-NASP antibody. *Lanes 3* and *4*, probed with anti-HSP90 antibody. *Lane 5*, control blot of HSP90 loaded onto the affinity column and eluted. Probed with anti-HSP90 antibody. *Lanes 6* and *7*, Amido Black stain. The lanes were loaded with equal amounts of protein. *cyt*, cytoplasmic fraction; *nucl*, nuclear fraction; *sNASP*, somatic/embryo form of NASP.

Affinity chromatography with anti-NASP antibodies confirmed the interaction between tNASP and HSP90 in mouse testis lysates (Fig. 5*A*). Moreover, as expected from the cross-linking studies of the HPLC (Bio-Sep SEC-S 3000 column) tNASP complexes, HSP90 was present in significant amounts (Fig. 5*A*). The distribution of tNASP and HSP90 in nuclear and cytoplasmic compartments was also studied to confirm the interaction between tNASP and HSP90 in mouse germ cells. As

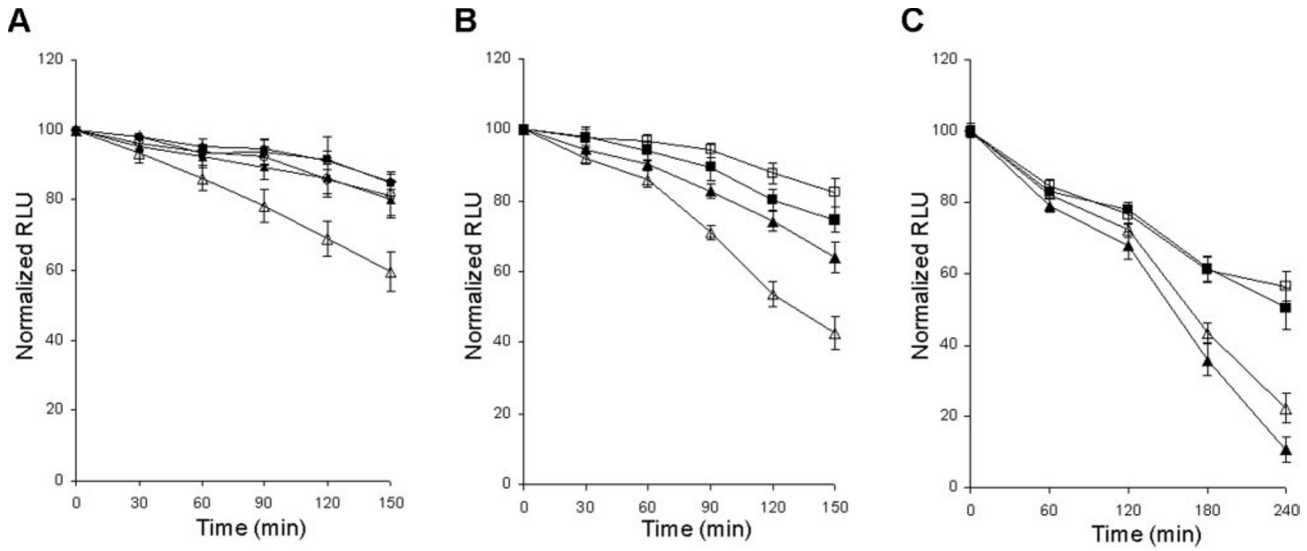

FIG. 6. **ATPase activity of HSP90.** *A*, ATPase activity of HSP90 is stimulated by tNASP. ◇, ATP alone; ■, ATP + tNASP; ▲, ATPase activity of HSP90+ATP; ○, ATPase activity of HSP90 + ATP in the presence of albumin; △, ATPase activity of HSP90 + ATP significantly increases ($p < 0.03$) with tNASP present. *B*, increasing concentrations of tNASP stimulate increasing ATPase activity of HSP90. ATP-HSP90 mixture was incubated with 0 (□), 0.1 (■), 0.2 (▲), and 0.4 μM (△) of tNASP. *C*, absence of tNASP TPR sites does not significantly reduce ATPase activity of HSP90. □, ATP only; ■, HSP90 + ATP; ▲, ATP-HSP90 mixture incubated with 0.4 μM of tNASP; △, ATP-HSP90 mixture incubated with 0.4 μM of tNASP-ΔTPR, mutant lacking the TPR sites. *RLU*, relative light unit(s).

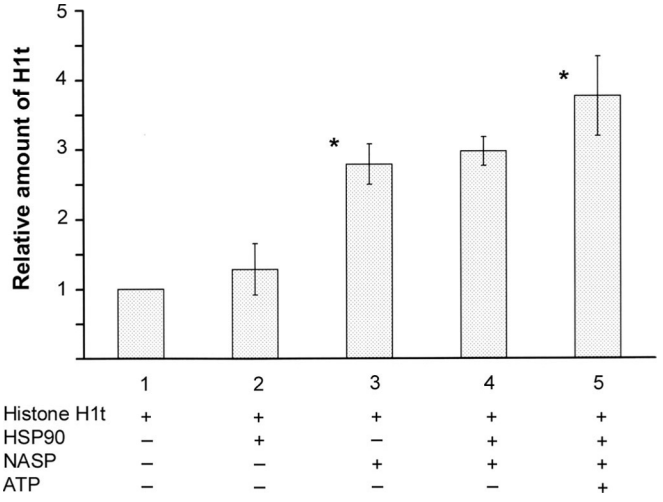

FIG. 7. **Co-immunoprecipitation of biotinylated H1t and tNASP by rabbit anti-NASP antibody with or without HSP90 and ATP.** The samples were separated by 10–20% SDS-PAGE, and the amount of co-immunoprecipitated H1t was calculated from background-subtracted images with gel imaging software. The relative amount of H1t is the average from four experiments. *Column 1*, nonspecific background binding. *Column 2*, nonspecific binding of H1t + HSP90. *Column 3*, binding of H1t to tNASP is significantly different ($p < 0.0007$) from the nonspecific binding of H1t to HSP90 (*column 2*). *Column 4*, binding of H1t to tNASP in the presence of HSP90. The presence of HSP90 does not significantly increase H1t binding (*column 3*). *Column 5*, binding of H1t to tNASP in the presence of HSP90 and 1 mM ATP. The presence of ATP significantly ($p < 0.04$) increases H1t binding to tNASP. The *error bars* represents ± S.D. The *asterisks* show significantly different amounts.

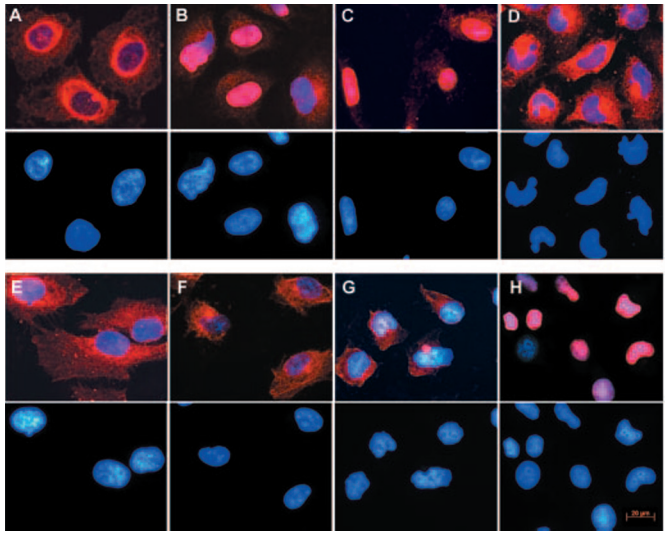

FIG. 8. **Nuclear transport of biotinylated linker histones in permeabilized HeLa cells.** The *top panels* show dual fluorescence of H1t (*A–F*) and H1s (*G* and *H*) detected by Texas Red avidin and nuclei by 4′,6′-diamino-2-phenylindole stain, and the *bottom panels* show only 4′,6′-diamino-2-phenylindole nuclear stain. All of the images were recorded with a Zeiss AxioCam through a 40× plan-neofluar 0.75 NA objective. The *scale bar* is 20 μm for all images. *A*, H1t histones at 37 °C are not detected within the nuclei. *B*, H1t histones at 37 °C in the presence of cytoplasmic extract are detected within nuclei. *C*, H1t histones at 37 °C in the presence of tNASP are transported into nuclei. *D*, under the energy deficient conditions of 4 °C there is no H1t nuclear transport. *E*, under the energy deficient conditions of no ATP there is no H1t nuclear transport. *F*, H1t histones at 37 °C in the presence of the nuclear localization signal deletion mutant (NASP-ΔNLS) are not transported into nuclei. *G*, somatic H1s at 37 °C are not detected within the nuclei. *H*, somatic H1s at 37 °C in the presence of tNASP are transported into nuclei.

shown in Fig. 5*B*, tNASP and HSP90 appear unequally distributed between nuclear and cytoplasmic fractions of mouse spermatogenic cells. Somatic NASP was present in small amounts in both nuclear and cytoplasmic fractions (Fig. 5*B*) and probably represents a contaminant from nonspermatogenic cells in testis. The quality of the nuclear and cytoplasmic preparations was monitored by the presence of histone H1 staining (Fig. 5*C*). Affinity chromatography with anti-NASP antibodies confirmed that the nuclear and cytoplasmic fractions of mouse germ cells contain tNASP (Fig. 5*D*, *lanes 1* and *2*). However, HSP90 co-purified with tNASP only from the cytoplasmic fraction (Fig. 5*D*, *lane 4*) and HSP90 alone did not bind to the anti-NASP affinity column (Fig. 5*D*, *lane 5*).

ATPase Activity of HSP90 Is Stimulated by tNASP—Nonactivated mammalian HSP90 has very low ATPase activity (23). The HSP90 ATPase activity, in the presence of ATP, was not significantly different from ATP alone or ATP + tNASP alone

TABLE I
Translocation of linker histones into HeLa cell nuclei

	Average number of cells counted ± S.D. ($n = 3$)	Average number of fluorescent nuclei ($n = 3$)	Percentage of fluorescent nuclei	Significance
H1t	247 ± 61.3	4.3 ± 1.5	2	
H1t + cytosol	232 ± 28.5	128.7 ± 14.8	55	$p < 0.005$
H1t + NASP	213 ± 37.5	137.7 ± 21.5	65	$p < 0.009$
H1t + NASP at 4 °C	250 ± 37.8	8.3 ± 7.1	3	$p < 0.006$ *vs.* NASP
H1t + NASP without ATP	243 ± 39.2	26.3 ± 10.6	11	$p < 0.005$ *vs.* NASP
H1t + NASP-ΔNLS	220 ± 18.7	6.3 ± 1.5	3	$p < 0.009$ *vs.* NASP
H1	221 ± 1.7	3 ± 2.7	1	
H1 + cytosol	258 ± 32.9	134.3 ± 44.5	52	$p < 0.04$
H1 + NASP	217 ± 29.5	148 ± 27.7	68	$p < 0.02$
H1 + NASP at 4 °C	259 ± 57.1	3 ± 0	1	$p < 0.012$ *vs.* NASP
H1 + NASP without ATP	217 ± 32.6	15 ± 2.7	7	$p < 0.014$ *vs.* NASP
H1 + NASP-ΔNLS	241 ± 62.2	10 ± 6.3	4	$p < 0.011$ *vs.* NASP

or ATP + HSP90 + bovine serum albumin (Fig. 6*A*). However, in the presence of tNASP the ATPase activity of HSP90 increased significantly (Fig. 6*A*; $p < 0.03$), and increasing amounts of tNASP (0.1, 0.2 and 0.4 μM) resulted in increasing HSP90 ATPase activity (Fig. 6*B*).

The presence of a TPR domain has been reported from a variety of proteins to interact with HSP90 (24). NASP contains TPR domains; therefore we tested a mutant tNASP lacking the TPR sites (NASP-ΔTPR). When the HSP90-ATP reaction mixture was incubated with NASP-ΔTPR, the HSP90 ATPase activity was strongly activated, although somewhat lower in activity than with intact tNASP (Fig. 6*C*). The tNASP TPR domains are apparently not required for the activation of HSP90 ATPase activity.

H1t Binding in the Presence of HSP90—Previous studies demonstrated that NASP binds somatic linker histones (9), and in the present study we have demonstrated that tNASP binds mouse testis-specific histone H1t. Because NASP stimulates HSP90 ATPase activity, we tested whether or not NASP binding H1t would increase in the presence of HSP90 and ATP. Fig. 7 demonstrates that the binding of H1t to NASP significantly increases in the presence of HSP90 and ATP ($p < 0.04$).

Nuclear Transport of Linker Histones by tNASP—Protein nuclear import requires soluble cytoplasmic factors (20), and linker histones may use importin β and importin 7 heterodimers for nuclear transport (25). However, tNASP has both a functional nuclear localization signal (10) and functional linker histone-binding sites (9). Therefore we tested the ability of tNASP to transport biotin-labeled H1t and somatic H1 histones into the nucleus utilizing an *in vitro* nuclear transport assay (20). As shown in Fig. 8 (*A*, *B*, and *G*) and Table I and as described previously (25), permeabilized HeLa cell nuclei do not transport H1 histones into the nucleus without the presence of cytoplasmic factors. Strikingly, tNASP (Table I) can completely replace the cytoplasmic factors and transport both H1t (Fig. 8*C*) and somatic H1 histones (Fig. 8*H*) into the nucleus. Transport by tNASP does not proceed at 4 °C (Fig. 8*D*), in the absence of ATP (Fig. 8*E*), or in the absence of the nuclear localization signal (Fig. 8*F*), indicating that transport is an energy-dependent process that requires the NLS.

DISCUSSION

In this study we have demonstrated that the histone-binding protein tNASP binds the testis-specific linker histone H1t and that the association of tNASP with HSP90 (identical to HSP86-1; accession number P07901) stimulated the ATPase activity of HSP90 and the binding of H1t to tNASP. We have shown that tNASP and HSP90 are present in both nuclear and cytoplasmic fractions of mouse germ cells; significantly HSP90 is bound to NASP only in the cytoplasm, leading to the conclusion that one function of HSP90 may be to chaperone the proper folding of NASP to bind linker histones. The timing of the stage-specific expression of HSP90, tNASP, and H1t supports the conclusion that the tNASP-H1t-HSP90 complex forms in the cytoplasm because HSP90 is expressed beginning on day 10 postpartum and approximately 2 days before the rapid increase in tNASP expression (Ref. 26; Mammalian Reproductive Genetics Data Base, *mrg.genetics.washington.edu/*). Expression of HSP90 and tNASP precede the expression of H1t in pachytene spermatocytes (13–15).

The activation of HSP90 ATPase activity by tNASP was similar to that reported for the specific activator Aha1 in yeast (27) and C143 in human cells (28). Surprisingly tNASP activation of HSP90 did not depend upon binding to any of the three TPR sites found in the C terminus of NASP. TPR sites have previously been reported (29) as protein-protein interaction sites between heat shock proteins and a number of functionally unrelated proteins. Our observation that NASP-HSP90 complexes occur only in the cytoplasm implies that there is a mechanism to release NASP from the complex. HSP90 can autophosphorylate serine (30) or threonine (23), and this has been proposed to control chaperone binding (31–34); therefore phosphorylation of HSP90 may regulate tNASP binding (35).

In addition to HSP90 ATPase activation and increased H1t binding, this study demonstrated that tNASP transports H1t as well as somatic H1 histones into the nucleus. Linker histones have not been reported to be free in the cytoplasm and with the help of HSP90 ATPase activity are likely to be immediately bound by tNASP upon completion of their synthesis in the cytoplasm. Released from the HSP90 complex, tNASP-H1t would then translocate to the nucleus using the NASP NLS, which has been shown to be necessary and sufficient for NASP transport into the nuclei of *Xenopus* oocytes (10). Linker histones do not have an NLS; however H1 histones can translocate into the nucleus in the presence of a cytoplasmic factor(s) (36) or importin β and importin 7 heterodimers (25), processes that are both temperature- and ATP-dependent. Similarly tNASP, in the absence of any other cytoplasmic factors, transports linker histones into the nucleus in an energy- and NLS-dependent manor. Consequently we hypothesize that after the synthesis of linker histones in the cytoplasm, they are bound to a complex containing NASP and HSP90, whose ATPase activity is stimulated by binding NASP. NASP-H1 is subsequently released from the complex and translocates to the nucleus where the H1 is released for binding to the DNA (8).

REFERENCES

1. Van Holde, K. E. (1989) *Chromatin*, Springer-Verlag, New York
2. Fan, Y., Nikitina, T., Morin-Kensicki, E. M., Zhao, J., Magnuson, T. R., Woodcock, C. L., and Skoultchi, A. I. (2003) *Mol. Cell. Biol.* **23,** 4559–4572
3. Cheung, E., Zarifyan, A. S., and Kraus, W. L. (2002) *Mol. Cell. Biol.* **22,** 2463–2471
4. Horn, P. J., Carruthers, L. M., Logie, C., Hill, D. A., Solomon, M. J., Wade, P. A., Imbalzano, A. N., Hansen, J. C., and Peterson, C. L. (2002) *Nat.*

Struct. Biol. **9,** 263–267
5. Brown, D. T., Alexander, B. T., and Sittman, D. B. (1996) *Nucleic Acids Res.* **24,** 486–493
6. Lever, M. A., Th'ng, J. P. H., Sun, X. J., and Hendzel, M. J. (2000) *Nature* **408,** 873–876
7. Misteli, T., Gunjan, A., Hock, R., Bustin, M., and Brown, D. T. (2000) *Nature* **408,** 877–881
8. Alekseev, O. M., Bencic, D. C., Richardson R. T., Widgren E. E., and O'Rand, M. G. (2003) *J. Biol. Chem.* **278,** 8846–8852
9. Richardson, R. T., Batova, I. N., Widgren, E. E., Zheng, L. X., Whitfield, M., Marzluff, W. F., and O'Rand, M. G. (2000) *J. Biol. Chem.* **275,** 30378–30386
10. O'Rand, M. G., Batova, I., and Richardson, R. T. (2000) in *The Testis: From Stem Cell to Sperm Function* (E. Goldberg, ed) pp. 143–150, Springer, New York
11. Richardson, R. T., Bencic, D. C., and O'Rand, M. G. (2001) *Gene* (*Amst.*) **274,** 67–75
12. Wang, Z-F., Sirotkin, A. M., Buchold, G. M., Skoultchi, A. I., Marzluff, W. F. (1997) *J. Mol. Biol.* **271,** 124–138
13. Meistrich, M. L., Bucci, L. R., Trostle-Weige, P. K., and Brock, W. A. (1985) *Dev. Biol.* **112,** 230–240
14. Drabent, B., Bode, C., Miosge, N., Herken, R., and Doenecke, D. (1998) *Cell Tissue Res.* **291,** 127–132
15. Grimes, S. R., Wilkerson, D. C., Noss, K. R., and Wolfe, S. A. (2003) *Gene* (*Amst.*) **304,** 13–21
16. Lin, Q., Inselman, A., Han, X., Xu, H., Zhang, W., Handel, M. A., and Skoultchi, A. I. (2004) *J. Biol. Chem.* **279,** 23525–23535
17. Bellve, A., Millette, C., Bhatnagar, Y., and O'Brien, D. (1977) *J. Histochem. Cytochem.* **25,** 480–494
18. O'Brien D. A. (1993) *Methods Toxicol.* **3A,** 246–264
19. Spector, D. L., Goldman, R. D., and Leinwand, L. A. (1998) *Cells: A Laboratory Manual*, p. 43.7, Cold Spring Harbor Laboratory, New York
20. Adam, S. A., Marr, R.S., and Gerace, L. (1990) *J. Cell Biol.* **111,** 807–816
21. Lea, I. A., Widgren, E. E., and O'Rand, M. G. (2004) *Reprod. Biol. Endocrinol.* **2,** 57
22. Brown, D. T., and Sittman, D. B. (1993) *J. Biol. Chem.* **268,** 713–718
23. Nadeau, K., Das, A., and Walsh, C. T. (1993) *J. Biol. Chem.* **268,** 1479–1487
24. Cheung-Flynn, J., Roberts, P., Riggs, D., and Smith, D. (2003) *J. Biol. Chem.* **278,** 17388–17394
25. Jakel, S., Albig, W., Kutay, U., Bishoff, F. R., Schwamborn, K., Doenecke, D., and Gorlich, D. (1999) *EMBO J.* **18,** 2411–2423
26. Shima, J. E., McLean, D. J., McCarrey, J. R., and Griswold, M. D. (2004) *Biol. Reprod.* **71,** 319–330
27. Meyer, P., Prodromou, C., Liao, C., Hu, B., Mark, R., Vauhgan, C., Vlasic, I., Panaretou, B., Piper, P., and Pearl, L. (2004) *EMBO J.* **23,** 511–519
28. Caplan, A., Jackson, S., and Smith, D. (2003) *EMBO Reports* **4,** 126–130
29. Blatch, G., and Lässle, M. (1999) *BioEssays* **21,** 932–939
30. Park, M., Young, K., and Krishna, P. (1998) *Mol. Cell. Biochem.* **185,** 33–38
31. Kim, H., Kang, K., Kang, H., and Kim, H. (1999) *J. Biochem.* (*Tokyo*) **126,** 1025–1032
32. Langer, T., Schlatter, H., and Fasold, H. (2002) *Cell Biol. Int.* **26,** 653–657
33. Csermely, P., Kajtar, J., Hollosi, M., Oikarinen, J., and Somogyi, J. (1994) *Biochem. Biophys. Res. Commun.* **202,** 1657–1663
34. Csermely, P., Miyata, Y., Schnaider, T., and Yahara, I. (1995) *J. Biol. Chem.* **270,** 6381–6388
35. Zhao, Y., Gilmore, R., Leone, G., Coffey, C., Weber, B., and Lee, P. (2001) *J. Biol. Chem.* **276,** 32822–32827
36. Kurz, M., Doenecke, D., and Albig, W. (1997) *J. Cell. Biochem.* **64,** 573–578